

Journal of Materials Chemistry B

Accepted Manuscript



This is an *Accepted Manuscript*, which has been through the Royal Society of Chemistry peer review process and has been accepted for publication.

Accepted Manuscripts are published online shortly after acceptance, before technical editing, formatting and proof reading. Using this free service, authors can make their results available to the community, in citable form, before we publish the edited article. We will replace this *Accepted Manuscript* with the edited and formatted *Advance Article* as soon as it is available.

You can find more information about *Accepted Manuscripts* in the [Information for Authors](#).

Please note that technical editing may introduce minor changes to the text and/or graphics, which may alter content. The journal's standard [Terms & Conditions](#) and the [Ethical guidelines](#) still apply. In no event shall the Royal Society of Chemistry be held responsible for any errors or omissions in this *Accepted Manuscript* or any consequences arising from the use of any information it contains.

Bioactive nanocomposites of bacterial cellulose and natural hydrocolloids

Cite this: DOI: 10.1039/x0xx00000x

Marco Aurelio Woehl,^a Lucy Ono,^b Izabel Cristina Riegel Vidotti,^a Fernando Wypych,^a Wido Herwig Schreiner^c and Maria Rita Sierakowski^a

Received ___ January 2012,
Accepted ___ January 2012

DOI: 10.1039/x0xx00000x

www.rsc.org/

The aim of this work was to develop bioactive films from bacterial cellulose and hydrocolloids (guar gum and hyaluronic acid), coated or not with collagen. After mechanical treatment, a suspension of cellulose nanofibres was obtained which, combined with the dispersions of hydrocolloids, was used to produce bionanocomposite films by wet casting. The materials were stable in physiological solution and presented better swelling capacity to that of the bacterial cellulose. The films were coated with collagen by dipping. Cell adhesion tests and surface analysis by tensiometry, X-ray photoelectron spectroscopy and atomic force microscopy showed that the surface properties of the films can be adjusted by changing the proportions of the components. The collagen coating presented a self-assembling pattern resembling that of living tissues. The materials developed in this work showed potential for applications in the medical field as bioactive wound dressings, scaffolds for cellular growth and sustained drug release systems. The films were obtained by simple production and purification methods, including the use of low toxicity solvents. Thus, in addition to potential cost saving, the development of these bionanocomposites is in accordance with Green Chemistry principles.

Introduction

The demand for biodegradable polymers to reduce environmental impacts has motivated the search for bionanocomposites, whose components have biological origin. Hydrocolloid-based composites have been studied for applications in the medical field,¹⁻³ particularly for the development of bioactive materials, which have an active influence on the inflammatory and cicatrisation processes and infection inhibition. This can be achieved through the release of drugs such as antibiotics, cell growth factor or nanoparticles with antibacterial action.⁴⁻¹⁰ Another approach complementary to drug release is to offer a surface on which controlled adhesion and proliferation of cells can occur.¹¹⁻¹³

The concept of bioactive material is not limited to topical applications. The so-called scaffolds act as supports to the proliferation of cells from the parent tissue, allowing its reconstitution.¹⁴ Among the processes for the production of nanostructured scaffolds are freeze casting, hydrocolloid mineralization and biomineralization by diffusion.¹⁵ These methods add to the already well-established methods of hydrocolloid freeze drying,⁷ nanofibre electrospinning¹² and direct injection of gels that biomimic the extracellular matrix.¹⁶

Galactomannans are polysaccharides with wide availability and low cost, although their use in release systems has not been widely investigated.^{17,18} Another promising application of

galactomannans is their adsorption on solid substrates for immobilization of biomolecules, which can allow the development of biosensors.^{19,20}

Hyaluronic acid (HA) is a polysaccharide with widespread medical applications. As a component of an extracellular matrix, it can be used in ophthalmic surgeries,²¹ tissue engineering²² and as a temporary substitute for skin in burn therapy.⁷ Due to its antioxidant properties, HA acts as an anti-inflammatory component in wound dressings.²³ However, its high cost has motivated the search for substitutes, *e.g.*, galactomannans.²⁴

Bacterial cellulose (BC) is another promising material for the development of bioactive composites, due to its biocompatibility and water retention properties. The main commercial application to the date is in the production of bioactive wound dressings.²⁵⁻²⁷ These dressings accelerate cicatrisation and reduce pain and the need for daily care of wounds. They maintain a humid environment around the wound, absorb the exudates and accommodate to the wound surface in nanoscale, thus contributing to cicatrisation and cellular regeneration. In second- and third-degree burns, BC membranes facilitate the clearance of necrotic residues and accelerate the reepitelisation process.²⁵

The first studies on the use of BC to form artificial blood vessels for microsurgery²⁸ called attention for BC's capability as a substrate for cell growth. The application of BC as

scaffolds for tissue regeneration has been investigated for cartilage,²⁹ muscle tissue,³⁰ skin tissue³¹ and, more frequently, bone tissue.^{3,14,15,32,33} Dental applications have also been studied.^{34,35}

The present work aims to combine the processability and versatility of composition of hydrocolloids with the biocompatibility and structural characteristics of BC. The process employed eliminates the usual need for covalent crosslinking in the production of hydrocolloid films and simplifies the preparation of a biocompatible collagen surface. The surface properties of the resulting materials were investigated to understand the factors related to cell adhesion and proliferation in the bionanocomposites' surfaces. The swelling behaviour of the materials in physiological solution was also investigated, aiming at *in vivo* applications.

Experimental

Materials

Never-dried membranes of *Gluconacetobacter xylinus* bacterial cellulose (BC) were supplied by Membracel Produtos Tecnológicos Ltda. (Almirante Tamandaré, PR, Brazil). Guar gum (lot # 098K0122), hyaluronic acid sodium salt (HA, from *Streptococcus equi*, lot #1420500 4279167) and collagen (type I, from bovine Achilles tendon, lot # 017K7018) were obtained from Sigma-Aldrich (Steinheim, Germany).

Prior to utilisation, the BC mats were kept in ultrapure water (MilliQ) under magnetic stirring in order to wash away any residual hypochlorite or sodium hydroxide left from the industrial purification process. The water was changed periodically until stable conductivity. The BC materials were homogenized in a kitchen blender and kept under refrigeration. The solids content was determined by drying weighed amounts of BC in a vacuum oven at 105 °C until constant weight.

The commercial guar gum was purified as follows. It was dispersed in water at 80 °C, and then left under magnetic stirring at 60 °C for 2 h and at 25 °C for 16 h. The resulting solution was centrifuged at 1000 g. The supernatant was dialysed against ultrapure water and freeze dried. The purified guar gum is therefore denominated GG. Hyaluronic acid, collagen and other chemicals were used without further purification.

Cytotoxicity assay

L929 mouse fibroblast cells were cultured in 96-well microplates and the monolayers were incubated with DMEM (200 µL) supplemented with 2% fetal bovine serum (FBS) containing 2-fold serial dilutions of hyaluronic acid or guar gum solutions, which were autoclaved by 121 °C for 15 min, prepared at different concentrations ranging from 0.0065 to 3.3 g.L⁻¹, and incubated for 72 h. The experiment was run in triplicate using 8 wells for each dilution. The *in vitro* toxicity of the compound was evaluated according to Denizot and Lang (1986) by quantifying the viable cells using 3-[4,5-dimethylthiazol-2-yl]-2,5-diphenyltetrazolium bromide (MTT), which is

converted into a coloured purple formazan by mitochondrial dehydrogenases. The 50% cytotoxic concentration (CC₅₀) was defined as the polysaccharide concentration that reduced the number of viable cells by 50% compared to a control without addition of polysaccharide. The cytotoxicity results were expressed as mean ± standard deviation, and analyzed by Student's *t*-test with *P*<0.01.

Preparation of the bionanocomposite films

The cellulose nanofibre suspension was obtained by mechanically dispersing the BC with an Ultra80 homogenizer (UltraStirrer, Brazil), at 22,000 RPM for 10 min. GG and HA were dispersed in water overnight to a concentration of 1% (w/w) of polysaccharide.

The BC suspension and the GG and HA dispersions were then mixed with the homogenizer at 5,000 RPM. The mixture was ultrasonicated to eliminate air bubbles, cast in polystyrene Petri dishes and dried at 37 °C for 48 h.

The GG:HA mass proportion was kept at 1:1 in all compositions. The resulting films were labelled BC50 to BC90, in which the numbers represent the BC dry mass percentage. A control film, BC100, was produced by casting only the BC dispersion.

Collagen deposition by dipping

A 0.1% (w/w) collagen dispersion in 0.1 mol.L⁻¹ acetic acid was prepared in an ice bath, with the aid of the Ultra80 homogenizer.

The bionanocomposite films were coated with collagen by a dipping method. The films were immersed in the collagen solution for 10 s, rinsed once with a 0.1 mol.L⁻¹ acetic acid solution, then twice with ultrapure water, and dried in a laminar flow chamber. Control films were submitted to the same procedure in solutions without collagen, in order to verify the effects of the procedure on the films' surface properties.

Swelling behaviour and stability in physiological solution

The films were cut in 10 mm diameter discs and immersed in physiological solution (0.9% aqueous NaCl) for determined periods of time and weighed, after removing the excess solution on the surface with and absorbing tissue. The mass uptake was calculated by the following equation:

$$m_U (\%) = 100 (m_w - m_i) / m_i$$

where m_U is the percentage of mass uptake, m_i is the initial mass of the films and m_w is the wet mass after the immersion.

The wet films were then dried at 37 °C for 48 h and weighed again to verify possible mass loss during immersion. The mass loss was corrected to account for the NaCl content in the liquid absorbed, according to the equation:

$$m_L (\%) = 100 [m_i - m_d + 0.009 (m_w - m_i)] / m_i$$

where m_L is the corrected mass loss, m_i is the initial mass of the

films, m_w is the wet mass after the immersion and m_d is the mass after drying.

Cell attachment assay

L929 mouse fibroblast cells were cultured on cell culture treated polystyrene (POL) as control, commercial bacterial cellulose (BC), BC100 and the bionanocomposites BC70, BC80 and BC90, in 24-well microplates at a concentration of 1.10^5 cells/well with DMEM (800 μ l) supplemented with 10% foetal bovine serum (FBS), and incubated for 72 h. Films were sterilized by UV irradiation for 60 min prior to the cell culture. The experiment was run in triplicate using 4 wells for each membrane. The *in vitro* attachment of L929 cells was evaluated by quantifying viable cells with the MTT method, described above. The percentage of viable cells was calculated in relation to the polystyrene control. The cell adhesion results were expressed as mean \pm standard deviation, and analyzed by Student's *t*-test with $P < 0.01$.

Surface characterization

Tensiometry. Contact angle (CA) analysis was performed in an OCA 15plus tensiometer (Dataphysics GmbH, Filderstadt, Germany), using the sessile drop method with ultrapure water. Measurements of CA were made at 25 °C using a 500- μ L Hamilton syringe (Bodanuz, Switzerland) and a needle with an internal diameter of 1.37 mm. The advancing contact angles were used to determine the surface free energy (SFE) of the material by the equation of state method.³⁶

X-ray photoelectron spectroscopy. XPS analysis was performed in an ESCA 3000 (VG Microtech, East Grinstead, UK) spectroscope with with Mg K_{α} and Al K_{α} radiation sources. Base pressure in the experimental chamber was lower than 10^{-9} mbar. The spectra were obtained at a takeoff angle of 45° using a hemispherical energy analyser with an overall energy resolution of 0.8 eV. The spectra were analyzed assuming core level spectra with line shapes with a Gaussian/Lorentzian ratio of 85/15, after standard Shirley background subtraction. Data were treated first by decomposing the carbon peak and then shifting the binding energy scale to bring the [C-O] component to 286.3 eV.

Microscopic characterisation

Scanning electron microscopy. SEM images were obtained using a VEGA3 LMU microscope (TESCAN Brno, s.r.o., Brno, Czech Republic) at 10 kV and at a magnification of 50,000 x. The samples were covered by a thin gold layer (<10 nm).

Atomic force microscopy. AFM was performed with an Agilent 550 microscope (Agilent Technologies, Santa Clara, CA, USA). Tapping mode and non-contact mode images were obtained with Mikromasch NSC35 probes (Nanoworld AG, Neuchâtel, Switzerland) with nominal spring constant of 14 N.m⁻¹ and resonance frequency of 150 kHz. The images were acquired with the Pico Image software (Agilent Technologies,

Santa Clara, CA, USA) and processed with the Gwyddion software (Czech Metrology Institute, Brno, Czech Republic).

Results and discussion

Cytotoxicity

The cytotoxicity to L929 cells was estimated by determining the percentage of surviving cells treated with the polysaccharides used to modify the cellulose membranes in comparison with a untreated control, after 72 h of incubation. Although hyaluronic acid has been widely used for biomedical applications and guar gum for food and cosmetic applications, their cytotoxicity was evaluated to exclude the potential toxicity to L929 cells, which were used in the biocompatibility experiments.

At the highest tested concentration (3.33 g.L⁻¹), hyaluronic acid (HA) decreased L929 cell viability by 23%, and by 17% at 1.67 g.L⁻¹, which resulted in a $CC_{50} > 3.33$ g.L⁻¹ (Fig. 1). This result was in accordance with the cytotoxicity values of HA for other cell lines, such as VERO, MDCK, MARK 145, PK15, which lowered the cellular viability by ~20% at 4 g.L⁻¹.³⁷

On the other hand, purified guar gum (GG) showed slightly lower cytotoxicity than HA, decreasing by 15% the number of viable cells at 3.33 g.L⁻¹, and no toxicity was observed up to 1.67 g.L⁻¹ (Fig. 1), which resulted in a $CC_{50} > 3.33$ g.L⁻¹.

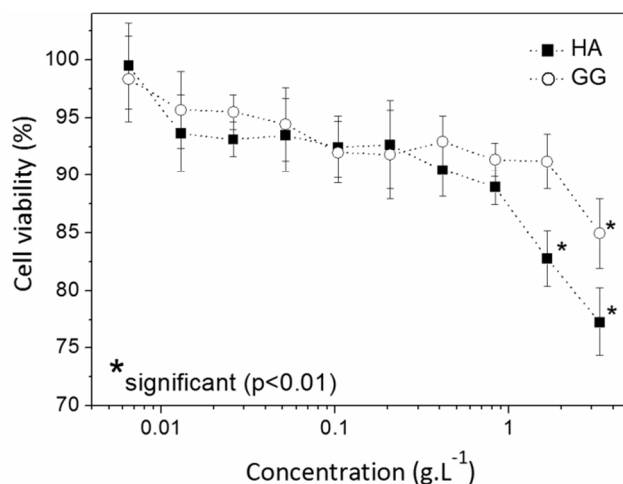


Fig. 1 Evaluation of cytotoxicity of hyaluronic acid (HA) and purified guar gum (GG) to L929 cells by the MTT assay, after 72 h of incubation at 37 °C and 5% CO₂. Control: without polysaccharide treatment. Vertical lines indicate standard deviations, n = 3, *p < 0.01.

As a food additive, guar gum has been considered safe for human consumption by the World Health Organization,³⁸ because no adverse effects were observed in rats at a dietary concentration of 5% administered in a long-term study of toxicity (24 months). Besides this safety information related to this use, there are few reports of the evaluation of guar gum toxicity in cell lines. These include the absence of guar gum cytotoxicity on human breast carcinoma cells (MCF-7) and human lymphoblastic leukaemia cells (1301),³⁹ and for nanoparticles of guar gum on human T-cell leukaemia cells (Jurkat) at the highest tested concentration of 150 μ M.⁴⁰

Considering that chitosan, poly(β -1,4-D-glucosamine), a polysaccharide approved for use in wound dressings, presents CC_{50} ranging from 0.21 to 2.50 $g.L^{-1}$,⁴¹ the high CC_{50} values obtained for hyaluronic acid and guar gum on L929 cells indicate a good potential for biocompatibility of cellulose membranes modified with these polysaccharides. The lowest CC_{50} value for guar gum compared to hyaluronic acid, whose use is approved for topical applications, supports the attempt to partially replace hyaluronic acid by guar gum on modified cellulose membranes in terms of safety.

Swelling behaviour and stability in physiological solution

The stability in physiological medium was the first criterion for selection of the bionanocomposite compositions suitable as substrates for cell adhesion and proliferation. In *in vivo* applications, e.g., as wound dressings, the films would be in contact with wound exudates that must be absorbed without loss of mechanical integrity. Most commercially available hydrocolloid dressings use covalent crosslinking to achieve stability.¹ Crosslinking is particularly important in collagen-based^{7,12,33} and hyaluronan-based systems,^{7,16,22,23} although it may raise concerns about cytotoxicity of the crosslinking agents and by-products.⁴² Therefore, the option here was to develop systems where the components are held together only by intermolecular interactions, reducing the use of potentially hazardous materials and the number of processing steps.

The swelling behaviour of the bionanocomposites is shown in Fig. 2. All the systems presented a fast initial swelling step (1 to 1.5 h) followed by contraction and slower swelling (days). A similar behaviour was observed by Elsner and Zilberman⁹ in a microporous system, where the first swelling step was attributed to a hydration effect. In the present materials, this step was much faster, indicating higher plasticity of the nanofibrillar network, probably due to the absence of crosslinking. The contraction step is due to an internal reorganization of the material, possibly with reaggregation of part of the nanofibres. The second swelling step was more intense in the films with 40 and 50% hydrocolloids (BC60 and BC50), leading to the disruption of the films during manipulation after 3 and 2 days, respectively. The liquid uptake of the films with lower hydrocolloid content stabilized after 1-2 days.

The expansion observed in the bionanocomposites, even those with low hydrocolloid content (BC80, BC90), is greater than the values reported in the literature⁹ and equivalent to lyophilized bacterial cellulose.⁴³ The percent mass uptake (m_U) of the bionanocomposites was related to their hydrocolloid content through a quadratic equation:

$$m_U(\%) = 295 + 1.88x + 0.279x^2 \quad (R^2 = 0.9885)$$

where x is the mass percent of hydrocolloids in the material. Therefore, the swelling characteristics of the bionanocomposites can be adjusted to suit different applications by changing the hydrocolloid content only.

The partial replacement of BC with HA and GG allowed greater absorption of water by the modified films. Moisture under dressing is a characteristic desired for wound dressings, since it accelerates epithelialisation and wound healing, by maintaining the proteins and cytokines produced in response to injury and facilitating autolytic debridement of the wound.⁴⁴

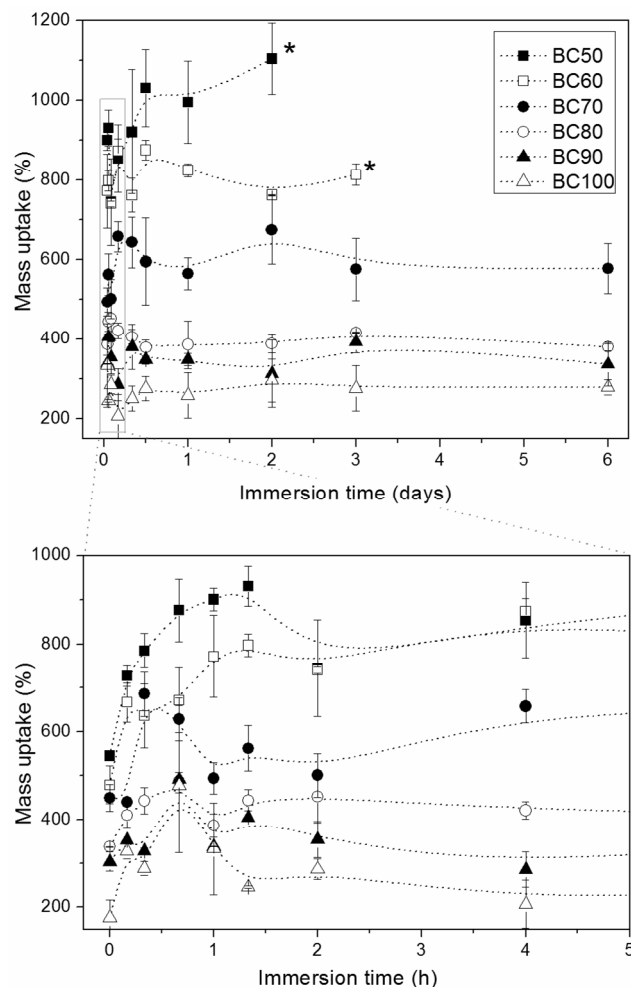


Fig. 2 Swelling behaviour in physiological solution of bionanocomposites with different cellulose contents (BC50-BC90) and reconstituted bacterial cellulose (BC100).

Fig. 3 shows the percent mass loss of the films when immersed in physiological medium. The already mentioned disruption of BC50 and BC60 films can be related to the mass loss presented in the first 24 h of immersion. On the other hand, the films with lower hydrocolloid content showed a mass loss close to the experimental error involved in the essay (*circa* $\pm 4\%$), when the results were corrected to account for the NaCl incorporated in the material during the test. Moreover, this stability in physiological medium was achieved without the need of chemical cross-linking of the polysaccharides. These results, combined with the low cytotoxicity observed in the hydrocolloids used, confirm the possibility of using the materials in topical applications.

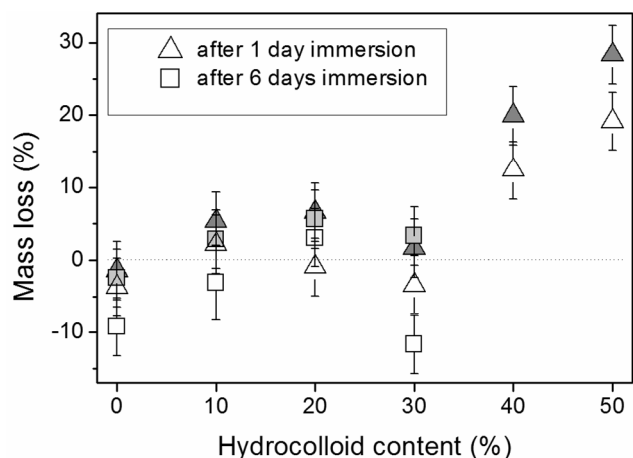


Fig. 3 Mass loss of the bionanocomposites after the swelling behaviour assays. Full symbols are the results corrected to account for the NaCl absorbed.

Cell adhesion

The cellular attachment assays showed there was no statistically significant difference ($P < 0.01$) among viable L929 cells on BC70, BC80 and BC (Fig. 4). Although all tested membranes showed significantly lower cellular viability in comparison to the polystyrene substrate (positive control), the results are showed here in comparison to the commercial BC. In terms of skin adhesion, BC is a porous adhesive wound dressing, which can be placed on skin without the need of secondary fixation. The porosity of BC allows better adhesion of the dressing on the skin, because it prevents the generation of air bubbles under the dressing and maximises the exudates draining from the wound, reducing the need to change the dressing.⁴⁵ Occlusive dressings that adhere aggressively to the wound can cause pain and inflammatory damage by skin stripping upon removal, which can be related to the quantity of skin cells attached.⁴⁶ Thus, the cell attachment results indicate that BC100, BC80 and BC70 could probably maintain this adhesion characteristic of BC.

Although the number of L929 cells attached on the bionanocomposites was similar to BC, the distribution of cells seemed to be more regular on BC80 and BC70 than on BC, which was characterized mainly by clusters with spheroid morphology cells (Fig. 5, circles), among large empty membrane spaces (arrows), although monolayer distribution of the cells on cell culture treated polystyrene was not achieved. This result indicates better homogeneity of the cell attachment on modified BCs in relation to unmodified BC. To the best of our knowledge, this is the first time that a guar-based surface is shown to be biocompatible and also that the GG can partially replace the HA, an already well-established bioactive compound, in substrates for cell growth.

The addition of collagen to the bionanocomposites led to differences in the morphology of L929 cells adhered to the films, without a statistically significant alteration of the number of viable cells (Fig. 4b). The BC deposited with collagen presented fibroblastic cells with spindle-shaped morphology

similar to that observed for L929 cells grown on polystyrene substrate, visualized by bright field microscopy (Fig. 5). Due to the higher opacity of the modified BCs deposited with collagen, the morphology of L929 cells attached to them was not clearly visualized, but as seen on BC, it suggested fibroblastic cells, since the tensiometry and XPS experiments indicated similar deposition of collagen on BC and modified BCs. The homogeneous distribution of the cells on modified BCs along with collagen was evidenced by the production of dark formazan by viable cells in the MTT assay.

This spreading of cells on collagen-coated BC was expected, since this protein is a constituent of the extracellular matrix, which functions as a support for cell adhesion, an important step for cell mobility, growth and viability.⁴⁷ Although this morphology of the cells seems to be advantageous to tissue organization, an *in vivo* evaluation is necessary to confirm whether it is capable of improving wound healing, since spreading also indicates greater strength of adhesion of the cells to the substrate. It has been reported that primary keratocytes of corneal stroma can grow in an attachment-independent manner, in the form of spheroid aggregates, under certain culture conditions, with more than 95% of the cells being viable.⁴⁸

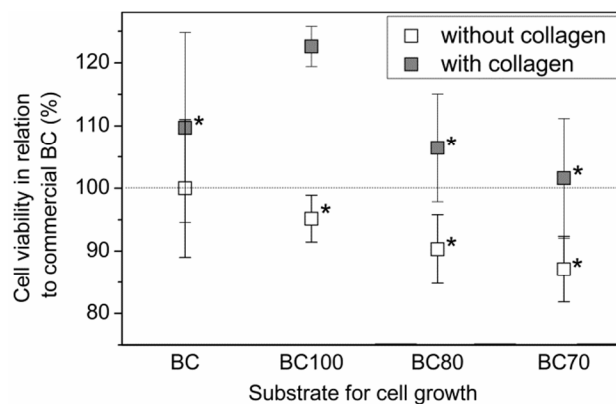


Fig. 4 Evaluation of L929 cell attachment on BC partially replaced by hyaluronic acid (HA) and guar gum (GG) 1:1, with and without deposited collagen, after 72 h of incubation at 37 °C and 5% CO₂ by the MTT assay. BC: commercial bacterial cellulose; BC100: bacterial cellulose cast from the cellulose nanofibre suspension; BC80: BC modified with 20% HA:GG replacement; BC70: BC modified with 30% HA:GG replacement. Bars represent means, with vertical lines indicating standard deviations, n = 3.

*no significant difference to non-coated BC ($P < 0.01$)

Furukawa, et al.⁴⁹ showed that spheroid aggregates of cells with low cell-substrate and high cell-cell interactions, obtained under specific conditions, cultured in a three-dimensional scaffold, produced a tissue-engineered skin with higher density of cells, which was expected to accelerate wound healing. They reported that the spheroid aggregates were able to produce a better expression of transforming growth factor - β_3 (TGF- β_3) mRNA, which accelerates wound healing, in comparison with the expression in spread fibroblast monolayers. Also, in

spheroid aggregates, cells seem to keep their differentiated phenotype, preserving the original cellular functions.⁵⁰

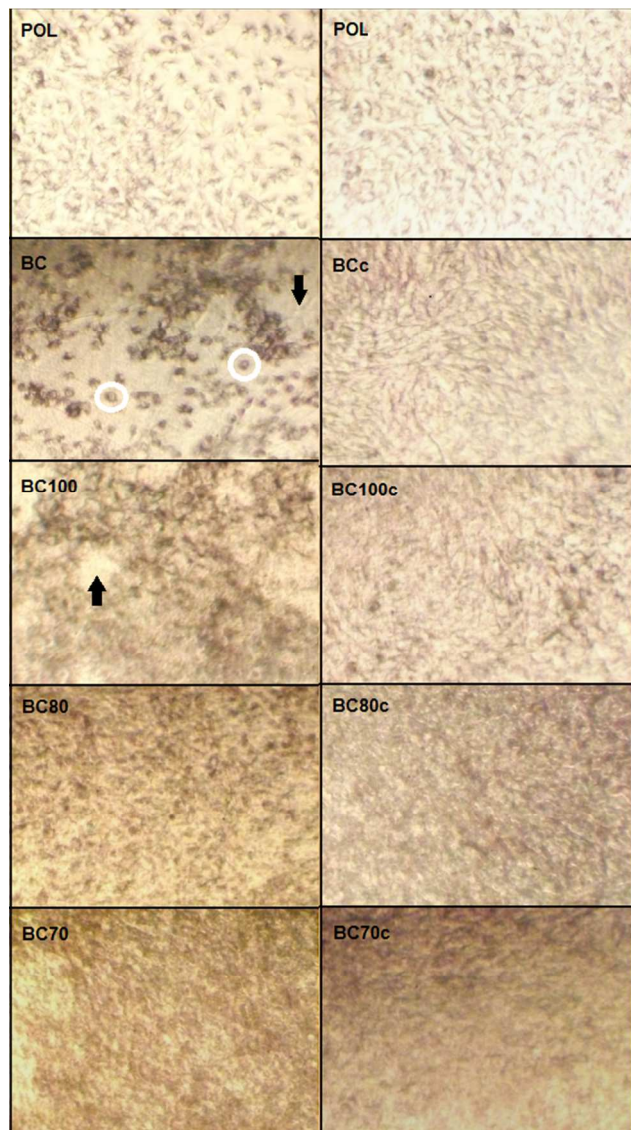


Fig. 5 Photomicrographs of the films without (left) and with collagen (right) evaluated for L929 cell attachment, after MTT assay. The morphology of the cells was observed by bright field microscopy with 200X magnification. Control: cell culture treated polystyrene substrate (POL); BC: commercial bacterial cellulose; BC100: reconstituted bacterial cellulose; BC80: BC with 20% HA:GG replacement; BC70: BC with 30% HA:GG replacement. Suffix c indicates collagen deposition. White circles: cells with spheroid morphology. Arrows: regions with no cell spreading.

On the other hand, Lei, et al.⁵¹ showed that mouse mesenchymal stem cells proliferated, spread and migrated differently on hyaluronic acid (HA) hydrogels, and, specifically related to the last characteristic, the 3% HA hydrogel with spindle-like cells migrated 95 $\mu\text{m}/\text{day}$ while 5% HA hydrogel with spherical cells migrated 0 $\mu\text{m}/\text{day}$. This could suggest a better migration rate for stem cells with the spread morphology. Wiegand, et al.⁵² reported that the incorporation of collagen on

bacterial cellulose membranes reduced the levels of proinflammatory interleukins, proteases and reactive species of oxygen, which are seen as advantageous characteristics for wound healing.

Tensiometry and surface free energy

The SFE results obtained for the cellulose surfaces, BC and BC100 (Fig. 6a) are in accordance with previously reported values. Cellulose SFE varies from 51.2 $\text{mN}\cdot\text{m}^{-1}$ for amorphous cellulose to 58.8 $\text{mN}\cdot\text{m}^{-1}$ for microcrystalline cellulose.^{53,54} The lowering of the SFE with the incorporation of the hydrocolloids is approximately linear and can be expressed by the equation:

$$\gamma_s = 56.2 - 0.358x \quad (R^2 = 0.9959)$$

where γ_s is the surface free energy and x is the mass percent of hydrocolloids in the materials. The relation between SFE and cell viability is also approximately linear for surfaces not coated with collagen (Fig. 6b). Since the SFE and surface wettability are among the factors that mediate cell adhesion/spreading on surfaces, with different cell lines displaying different behaviours,^{13,55,56} this result shows yet another set of properties that can be adjusted in these materials by the modification of the components' proportion.

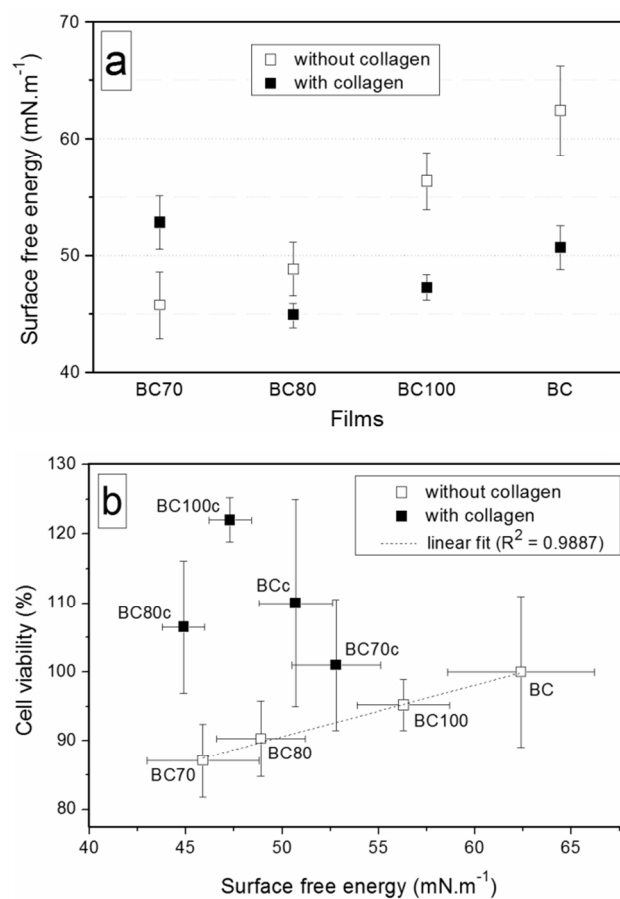


Fig. 6 (a) Surface free energy of commercial bacterial cellulose

(BC), reconstituted bacterial cellulose (BC100) and bionanocomposites BC70 and BC80, before and after collagen deposition; (b) cell viability versus surface free energy for the same materials.

The SFE of the surfaces coated with collagen (Fig. 6a) were in a narrower range, which is compatible with the values found by Harnett, et al.⁵⁷ for different collagen-coated surfaces. However, there is no obvious trend in the SFE variation as observed in the uncoated surfaces. The BC70 film showed a SFE higher than the BC80, which suggests that some other factor than the surface composition plays a role in the SFE. There was no clear relationship either between SFE and cell viability in the collagen-coated films (Fig. 6b). These results show the need to investigate the surface properties of the material to find another factor mediating cell adhesion.

Microscopic characterisation

The SEM images of the reconstituted BC and bionanocomposites (Fig. 7) are nearly indistinguishable from each other, showing the same mesh-like pattern. No regions of hydrocolloid segregation were observed, with the bionanocomposites retaining the original morphology of the surface in spite of the different composition. The hydrocolloids are therefore spread evenly on the surface of the cellulose nanofibres.

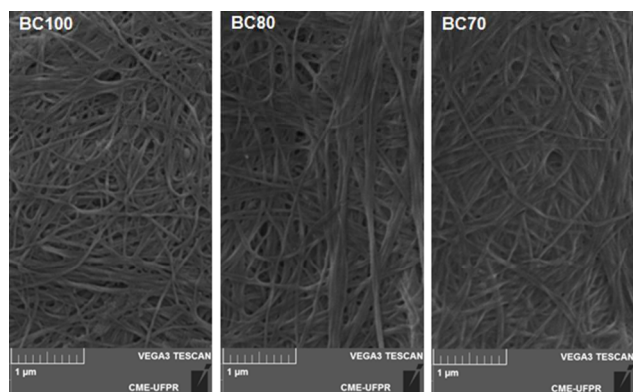


Fig. 7 SEM images of the reconstituted bacterial cellulose (BC100) and the bionanocomposites BC80 and BC70.

Comparing the AFM images of the BC100 and BC70 surfaces (Fig. 8) revealed some important differences. In the BC100 image, there are scanning artefacts (arrows) that reveal a mobility of the nanofibres, a feature not observed in the bionanocomposite image. The corresponding phase angle histogram of those images showed a wider angle distribution for the BC100, which confirms that the BC nanofibres are loosely associated. In the BC70, however, the angle distribution is much narrower, suggesting mechanical stabilization promoted by the hydrocolloids. Moreover, the angle distribution is monomodal, showing a homogeneous surface and confirming that the surface is evenly covered by the hydrocolloids.

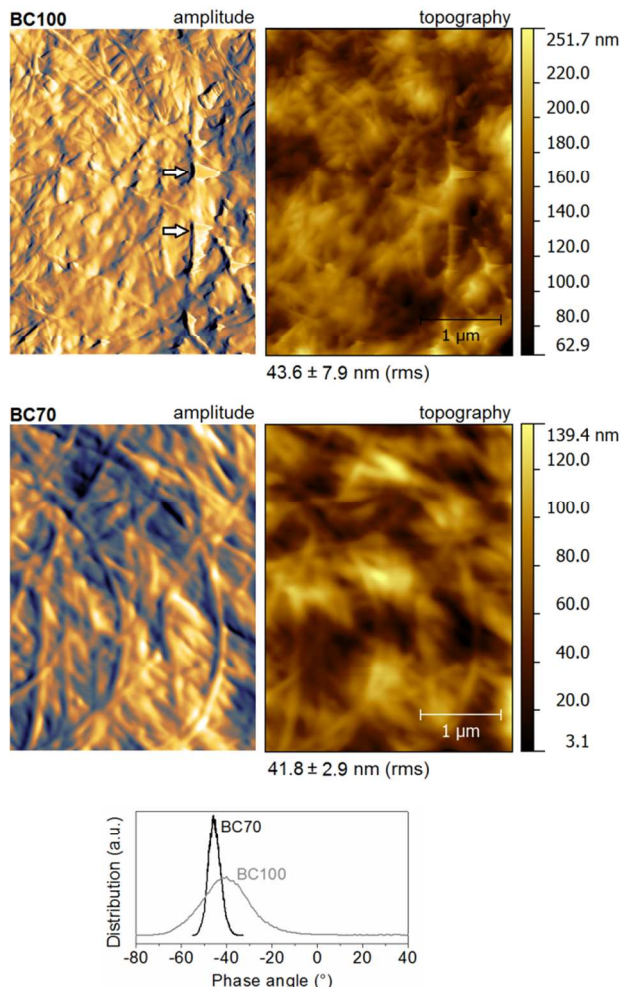


Fig. 8 AFM tapping mode images of the reconstituted bacterial cellulose (BC100), the bionanocomposite BC70 and respective phase angle histograms.

The coating of the surface with collagen led to modification of surface patterns (Fig. 9). In the BC100, although there was a suggestion of collagen self-assembly, no clear pattern was observed. On the other hand, the BC70 surface promoted the self-assembly of collagen microfibrils with a repetition pattern of 64.8 ± 5.4 nm, characteristic of type I collagen.⁵⁸ Although Bet, et al.⁵⁹ obtained a similar surface pattern, it was achieved by chemical modification of the collagen. The width of the microfibrils observed here, up to 561 nm, is also larger than those of the mentioned work. The microfibrils organized in a tape-like pattern, different from the circular section fibrils observed when collagen polysaccharides induce the collagen self-assembling in solution.⁶⁰ The higher degree of organization of the collagen in the hydrocolloid-loaded composites may explain the more homogeneous spreading of the fibroblast cells in comparison with the BC100c composite, since the collagen is in a conformation similar to that observed in the extracellular medium.⁶¹

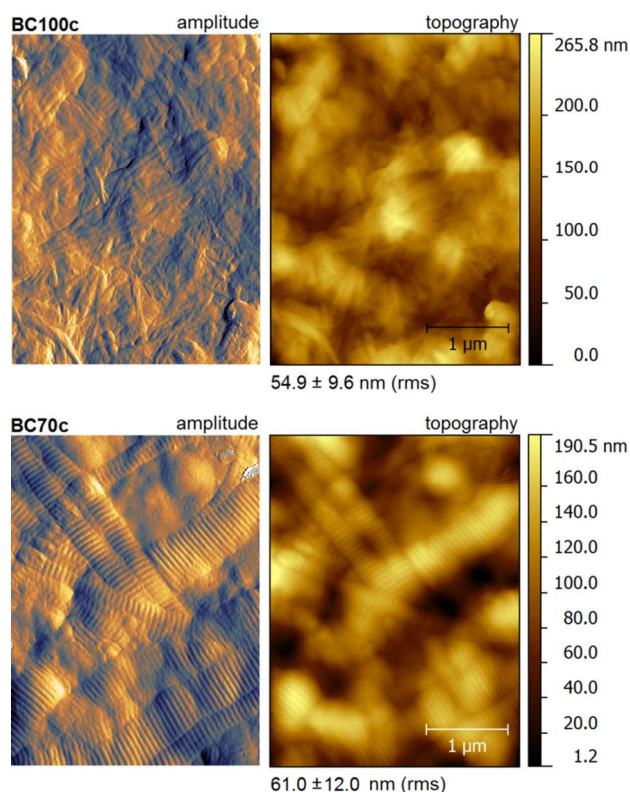


Fig. 9 AFM tapping mode images of the collagen-coated reconstituted bacterial cellulose (BC100c) and collagen-coated bionanocomposite BC70c.

The collagen coating increased the rugosity of the surfaces (Fig. 8 and 9), with the BC70 showing the highest increase upon collagen deposition. Both the increase of rugosity and the collagen self-assembly, which may expose different functional groups, should contribute to the higher SFE presented by the BC70 film.

X-ray photoelectron spectroscopy

Figure 10 shows the C 1s high resolution spectra of the bionanocomposites, as well as films cast from suspensions of their individual components. The BC100 shows a contribution from adventitious carbon, [C-C], in a level usually found in high purity cellulose standards.⁶² The proportion between the [C-OH] and [O-C-O] contributions is very close to the 3:1 proportion theoretically expected for cellulose. The low resolution XPS survey of BC100 (data not shown) revealed only a small nitrogen contribution ($N/C = 0.020$), confirming the high purity of the cellulose used in the materials.

The C 1s profiles of the bionanocomposites resemble more closely those of the hydrocolloids (HA and GG) than that of the cellulose. Table 1, besides the experimental values found for the different carbon contributions, reports the estimated contributions for surfaces completely covered with the HA:GG mixture and surfaces in which there is exposure of 10% of the cellulose substrate. These estimations were made by linear combinations of the experimental values from the individual

components HA, GG and BC100. It can be seen that the bionanocomposites agree well with a surface completely covered with hydrocolloids or, at most, with 10% contribution of cellulose.

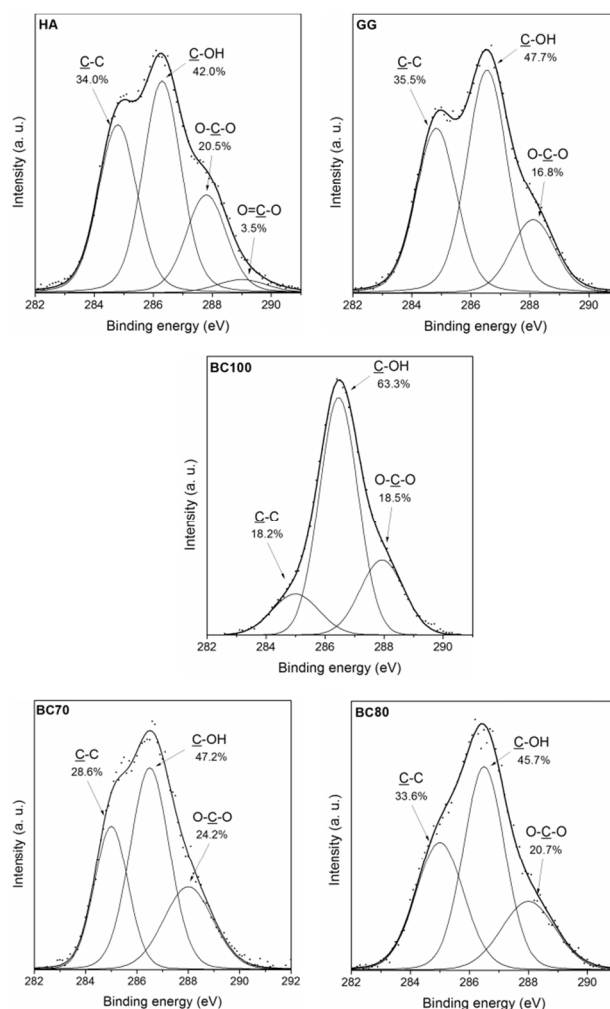


Fig. 10 High resolution XPS C 1s spectra of hyaluronic acid (HA), purified guar gum (GG), reconstituted bacterial cellulose (BC100) and the bionanocomposites BC70 and BC80.

The only feature not consistent with this prediction is the [O=C-O] contribution in the bionanocomposites, which was below the limit of detection of the equipment (less than 1%) and therefore was not considered in the final peak fitting. To further investigate the carboxyl group contribution on the surfaces, we analysed the O 1s peaks (Fig. 11). In the HA, we found a peak with binding energy of 531.2 eV, assigned to carboxylate (COO^-), and amide ($\text{O}=\text{C}-\text{N}$),⁶³ too close to be deconvoluted. The main peak (532.7 eV), corresponding to hemiacetal and hydroxyl groups, is in a proportion close to the theoretical 8:3 (73:27 %) expected for the sodium salt form of HA. The presence of the Na KLL Auger peak reinforces the idea that HA is in the sodium salt form.

Table 1 Experimental C 1s XPS contributions for the purified guar gum (GG), reconstituted bacterial cellulose (BC100) and the bionanocomposites BC70 and BC80; contributions estimated for surfaces with different BC, HA and GG contents.

FILM	Atomic %			
	C-C	C-OH	O-C-O	O=C-O
Experimental				
GG	35.5	47.7	16.8	*
HA	34.0	42.0	20.5	3.5
BC100	18.2	63.3	18.5	*
BC80	33.6	45.7	20.7	*
BC70	28.6	47.2	24.2	*
Estimated				
Total coating by HA:GG	34.7	44.8	18.7	1.8
10% exposure of BC surface	33.1	46.7	18.6	1.6

*Below the limit of detection of the equipment (less than 1%)

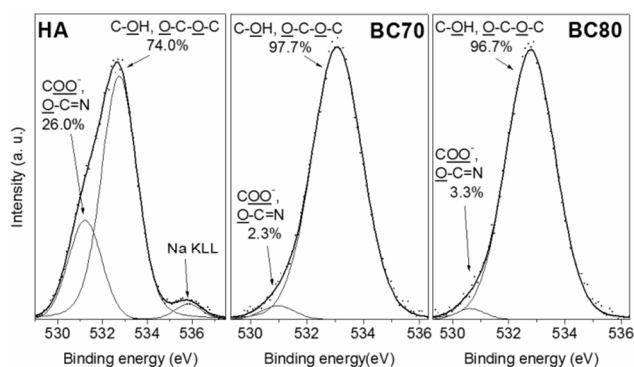


Fig. 11 High-resolution XPS O 1s spectra of hyaluronic acid (HA) and the bionanocomposites BC70 and BC80.

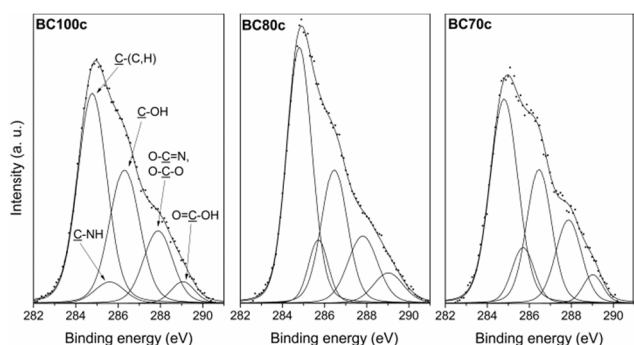


Fig. 12 High-resolution XPS C 1s spectra of collagen-coated reconstituted bacterial cellulose (BC100c) and bionanocomposites BC70c and BC80c. The peak intensities were normalized in relation to the C-OH component.

However, the contribution of the 531.2 eV peak in the bionanocomposites is much smaller than expected from the HA content in the films. One may conclude that the carboxyl

groups are oriented away from the film surface, possibly interacting with the cellulose surface. This could explain the lower hydrophilicity observed for the bionanocomposites by the tensiometry assays, which is unexpected considering the high water retention capacity of HA.

The collagen deposition on the films drastically changed the C 1s peak profile (Fig. 12). The peaks are very similar, independent of the used substrate. Since collagen has a much more complex structure than the polysaccharides in the substrate, the peak deconvolution is not straightforward. The most applied option is the deconvolution in three peaks, as adopted by Côté, et al.⁴ and Gurdak, et al.⁶⁴, with the binding energies of 284.8 eV for C-(C,H), 286.3 eV for C-(O,N) and 288 eV for amide carbon, O=C=N. However, it is possible to assign the latter peak to amide hemiacetal carbons and split the former in a C-NH component, at 285.7 eV, and a C-OH component at 286.3 eV, adding also a peak at 289.0 eV for carboxyl carbon. The resulting fit, shown in Fig. 12, is very close to the C 1s profiles of collagen- and gelatin-coated surfaces⁶⁵⁻⁶⁷, which show slight differences (± 0.2 eV) in the reported peak energies due to different energies assigned to the C-(C,H) binding energy.

If the C-(C,H) peak, which is prone to adventitious carbon contamination, is dismissed, the relative proportions of the remaining peaks in both the BC70c and BC80c composites is very close to other works⁶⁵⁻⁶⁷. In the BC100c composite, however, there is an increase in the C-OH peak in relation to the C-NH peak, which indicates a contribution of the polysaccharide substrate. This may be due to a lower density of the less organized collagen layer (as observed in the AFM images) or to a less effective coating.

As already reported by Gurdak, et al.⁶⁴, the N/C molar ratio determined by XPS in protein films is systematically smaller than that obtained by elemental analysis. In the present case, the N/C molar ratios were 0.114, 0.103 and 0.097 for BC70c, BC80c and BC100c, respectively. The N/O molar ratios are more reliable, since they are not influenced by the presence of adventitious carbon contamination. In the composites not coated with collagen, the N/C ratios were 0.065, 0.043 and 0.027 for BC70, BC80 and BC100, respectively, reflecting the decreasing HA content. The collagen coating elevates the N/C ratios to 0.278, 0.292 in the BC70c and BC80c films, values very close to the obtained for the pristine collagen (0.284). The BC100c film has a 0.248 N/C ratio, due to the already mentioned contribution of the substrate to the XPS signal.

Conclusions

The bionanocomposites described here have high water retention capacity and are stable under physiological conditions, without the need for crosslinking reactions of the hydrocolloids utilised. The liquid uptake of the bionanocomposites in physiological medium showed a relation with the hydrocolloid content, which allows adjusting the swelling properties of the materials. The systems with hydrocolloid content of 30% or less presented low mass loss upon hydration, which combined with the low cytotoxicity of

the polysaccharides employed allows applications *in vivo* or *in vitro* where the materials are in contact with physiological medium.

The adhesion and proliferation of mouse fibroblasts on the bionanocomposites' surfaces was equivalent to that of the commercial bacterial cellulose, with the advantage of more homogenous cell spreading. The morphology of the adhered cell indicated an environment favourable to fibroblast development. There was a relation between the surface-free energy and the cell viability, as well as between the surface-free energy and the hydrocolloid content. Therefore, these properties can also be adjusted by changing the hydrocolloid content.

The collagen deposition by a simple dipping procedure was very effective, with a homogenous coating. The collagen coating increased cell viability in all the compositions. The hydrocolloids induced the self-assembling of collagen on the surfaces, in a pattern resembling that observed in living tissues.

The materials developed in this work showed potential for applications in the medical field as bioactive wound dressings and scaffolds for cellular growth. The films were obtained by simple production and purification methods, including the use of low toxicity and easily recovered solvents. Thus, in addition to potential cost savings, the development of these bionanocomposites is in accordance with the Green Chemistry principles.

Acknowledgements

We acknowledge support from the Brazilian funding agencies CAPES and CNPq, and the help of the Electron Microscopy Centre, CME/UFPR for the SEM images. We are also grateful to Membracel Produtos Tecnológicos Ltda. for the bacterial cellulose samples.

Notes and references

^aBioPol, Departamento de Química, ^bDepartamento de Patologia Básica and ^cDepartamento de Física, Universidade Federal do Paraná (UFPR), P.O. 19081, Curitiba 81531-980, PR, Brazil.

- 1 J. S. Boateng, K. H. Matthews, H. N. E. Stevens and G. M. Eccleston, *Journal of Pharmaceutical Sciences*, 2008, **97**, 2892-2923.
- 2 D. Campoccia, L. Montanaro and C. R. Arciola, *Biomaterials*, 2013, **34**, 8533-8554.
- 3 D. Puppi, F. Chiellini, A. M. Piras and E. Chiellini, *Progress in Polymer Science*, 2010, **35**, 403-440.
- 4 M.-F. Côté, G. Laroche, E. Gagnon, P. Chevallier and C. J. Doillon, *Biomaterials*, 2004, **25**, 3761-3772.
- 5 Z. Dong, Q. Wang and Y. Du, *Journal of Membrane Science*, 2006, **280**, 37-44.
- 6 M. H. El-Rafie, A. A. Mohamed, T. I. Shaheen and A. Hebeish, *Carbohydrate Polymers*, 2010, **80**, 779-782.
- 7 S. N. Park, J. K. Kim and H. Suh, *Biomaterials*, 2004, **25**, 3689-3698.
- 8 C. Wiegand, T. Heinze and U.-C. Hipler, *Wound Repair and Regeneration*, 2009, **17**, 511-521.
- 9 J. J. Elsner and M. Zilberman, *Journal of Tissue Viability*, 2010, **19**, 54-66.
- 10 L. Huang, X. Chen, T. X. Nguyen, H. Tang, L. Zhang and G. Yang, *Journal of Materials Chemistry B*, 2013, **1**, 2976-2984.

- 11 W. Y. Huang, C. L. Yeh, J. H. Lin, J. S. Yang, T. H. Ko and Y. H. Lin, *Journal of materials science. Materials in medicine*, 2012, **23**, 1465-1478.
- 12 S. Zhong, W. E. Teo, X. Zhu, R. W. Beuerman, S. Ramakrishna and L. Y. L. Yung, *Journal of Biomedical Materials Research Part A*, 2006, **79A**, 456-463.
- 13 S. B. Kennedy, N. R. Washburn, C. G. Simon Jr. and E. J. Amis, *Biomaterials*, 2006, **27**, 3817-3824.
- 14 S. Bose, M. Roy and A. Bandyopadhyay, *Trends in Biotechnology*, 2012, **30**, 546-554.
- 15 E. Saiz, E. A. Zimmermann, J. S. Lee, U. G. K. Wegst and A. P. Tomsia, *Dental materials : official publication of the Academy of Dental Materials*, 2013, **29**, 103-115.
- 16 M. W. Lee and K. Y. Tung, *Biomedical Engineering: Applications, Basis and Communications*, 2010, **22**, 401-407.
- 17 T. Coviello, F. Alhaique, A. Dorigo, P. Matricardi and M. Grassi, *European Journal of Pharmaceutics and Biopharmaceutics*, 2007, **66**, 200-209.
- 18 T. Coviello, P. Matricardi, C. Marianecchi and F. Alhaique, *Journal of Controlled Release*, 2007, **119**, 5-24.
- 19 M. R. Sierakowski, R. A. Freitas, J. Fujimoto and D. F. S. Petri, *Carbohydrate Polymers*, 2002, **49**, 167-175.
- 20 F. Valenga, D. F. S. Petri, N. Lucyszyn, T. A. Jó and M. R. Sierakowski, *International Journal of Biological Macromolecules*, 2012, **50**, 88-94.
- 21 F. Guillaumie, P. Furrer, O. Felt-Baeyens, B. L. Fuhendorff, S. Nymand, P. Westh, R. Gurny and K. Schwach-Abdellaoui, *Journal of Biomedical Materials Research Part A*, 2010, **92A**, 1421-1430.
- 22 C. Fan, L. Liao, C. Zhang and L. Liu, *Journal of Materials Chemistry B*, 2013, **1**, 4251-4258.
- 23 G. Kogan, L. Soltes, R. Stern and P. Gemeiner, *Biotechnology Letters*, 2007, **29**, 17-25.
- 24 R. R. Castro, J. P. A. Feitosa, P. L. R. da Cunha and F. A. C. da Rocha, *Clinical Rheumatology*, 2007, **26**, 1312-1319.
- 25 W. Czaja, A. Krystynowicz, S. Bielecki and R. M. Brown, *Biomaterials*, 2006, **27**, 145-151.
- 26 J. D. Fontana, A. M. Desouza, C. K. Fontana, I. L. Torriani, J. C. Moreschi, B. J. Gallotti, S. J. Desouza, G. P. Narcisco, J. A. Bichara and L. F. X. Farah, *Appl Biochem Biotech*, 1990, **24-5**, 253-264.
- 27 N. Shah, M. Ul-Islam, W. A. Khattak and J. K. Park, *Carbohydrate Polymers*, 2013, **98**, 1585-1598.
- 28 D. Klemm, D. Schumann, U. Udhardt and S. Marsch, *Progress in Polymer Science*, 2001, **26**, 1561-1603.
- 29 A. Svensson, E. Nicklasson, T. Harrah, B. Panilaitis, D. L. Kaplan, M. Brittberg and P. Gatenholm, *Biomaterials*, 2005, **26**, 419-431.
- 30 H. Bäckdahl, G. Helenius, A. Bodin, U. Nannmark, B. R. Johansson, B. Risberg and P. Gatenholm, *Biomaterials*, 2006, **27**, 2141-2149.
- 31 L. Fu, Y. Zhang, C. Li, Z. Wu, Q. Zhuo, X. Huang, G. Qiu, P. Zhou and G. Yang, *Journal of Materials Chemistry*, 2012, **22**, 12349-12357.
- 32 M. Zaborowska, A. Bodin, H. Bäckdahl, J. Popp, J. Goldstein and P. Gatenholm, *Acta Biomaterialia* 2010, **6**, 2540-2547.

- 33 S. Saska, L. N. Teixeira, P. Tambasco de Oliveira, A. M. Minarelli Gaspar, S. J. Lima Ribeiro, Y. Messaddeq and R. Marchetto, *Journal of Materials Chemistry*, 2012, **22**, 22102-22112.
- 34 G. M. Olyveira, G. A. X. Acasigua, L. M. M. Costa, C. R. Scher, L. Xavier, P. H. L. Pranke and P. Basmaji, *J. Biomed. Nanotechnol.*, 2013, **9**, 1370-1377.
- 35 L. Catalfamo, E. Belli, C. Nava, E. Mici, A. Calvo, B. Alessandro and F. S. De Ponte, *International Journal of Nanomedicine*, 2013, **2013**, 3883-3886.
- 36 A. W. Neumann, R. J. Good, C. J. Hope and M. Sejpal, *Journal of Colloid and Interface Science*, 1974, **49**, 291-304.
- 37 C. Cermelli, A. Cuoghi, M. Scuri, C. Bettua, R. G. Neglia, A. Ardizzoni, E. Blasi, T. Iannitti and B. Palmieri, *Virology Journal*, 2011, **8**, 1-8.
- 38 *Toxicological evaluation of some food colours, thickening agents, and certain other substances*, Report n. 55A, WHO – World Health Organization, 1975.
- 39 A. M. Gamal-Eldeen, H. Amer and W. A. Helmy, *Chemico-Biological Interactions*, 2006, **161**, 229-240.
- 40 J. K. Sarmah, R. Mahanta, S. K. Bhattacharjee, R. Mahanta, A. Dey, P. Guha and A. Biswas, *Journal of drug delivery & Therapeutics*, 2012, **2**, 67-71.
- 41 T. Kean and M. Thanou, *Advances in Drug Delivery Reviews*, 2010, **62**, 3-11.
- 42 C. Englert, T. Blunk, R. Muller, S. S. von Glasser, J. Baumer, J. Fierbeck, I. M. Heid, M. Nerlich and J. Hammer, *Arthritis Res. Ther.*, 2007, **9**, R47.
- 43 D. Klemm, B. Heublein, H. P. Fink and A. Bohn, *Angew Chem Int Edit*, 2005, **44**, 3358-3393.
- 44 V. Jones, J. E. Grey and K. G. Harding, *British Medical Journal*, 2006, **332**, 777-780.
- 45 J. C. Vieira, A. Z. Badin, L. H. Calomeno, V. Teixeira, E. Ottoboni, M. Bailak and G. Salles Jr., *Arquivos Catarinenses de Medicina*, 2007, **36**, 94-97.
- 46 M. Waring, M. Rippon, S. Bielfeldt and M. Brandt, *Wounds UK*, 2008, **4**, 35-47.
- 47 A. Gaspar, L. Moldovan, D. Constantin, A. M. Stanciu, P. M. Sarbu-Boeti and I. C. Efrimescu, *Journal of Medicine and Life*, 2011, **4**, 172-177.
- 48 M. L. Funderburgh, M. M. Mann and J. L. Funderburgh, *Molecular Vision*, 2008, **14**, 308-317.
- 49 K. S. Furukawa, T. Ushida, Y. Sakai, K. Kunii, M. Suzuki, J. Tanaka and T. Tateishi, *Journal of Artificial Organs*, 2001, **4**, 353-356.
- 50 W. F. Liu and C. S. Chen, *Advances in Drug Delivery Reviews*, 2007, **59**, 1319-1328.
- 51 Y. Lei, S. Goigini, J. Lam and T. Segura, *Biomaterials*, 2011, **32**, 39-47.
- 52 C. Wiegand, P. Elsner, U.-C. Hipler and D. Klemm, *Cellulose*, 2006, **13**, 689-696.
- 53 C. Aulin, S. Ahok, P. Josefsson, T. Nishino, Y. Hirose, M. Österberg and L. Wågberg, *Langmuir : the ACS journal of surfaces and colloids*, 2009, **25**, 7675-7685.
- 54 D. J. Gardner, G. S. Oporto, R. Mills and M. A. S. A. Samir, *Journal of Adhesion Science and Technology*, 2008, **22**, 545-567.
- 55 T. G. Ruardy, H. E. Moorlag, J. M. Schakenraad, H. C. Van Der Mei and H. J. Busscher, *Journal of Colloid and Interface Science*, 1997, **188**, 209-217.
- 56 C. Jin, Y. Jiang, T. Niu and J. Huang, *Journal of Materials Chemistry*, 2012, **22**, 12562-12567.
- 57 E. M. Harnett, J. Alderman and T. Wood, *Colloids and Surfaces B: Biointerfaces*, 2007, **55**, 90-97.
- 58 K. E. Kadler, D. F. Holmes, J. A. Trotter and J. A. Chapman, *Biochemistry Journal*, 1996, **316**, 1-11.
- 59 M. R. Bet, G. Goissis, S. Vargas and H. S. Selistre-de-Araujo, *Biomaterials*, 2003, **24**, 131-137.
- 60 S.-W. Tsai, R.-L. Liu, F.-Y. Hsu and C.-C. Chen, *Biopolymers*, 2006, **83**, 381-388.
- 61 S. Richard-Blum and F. Ruggiero, *Pathologie Biologie*, 2005, **53**, 430-442.
- 62 L.-S. Johansson and J. M. Campbell, *Surface and Interface Analysis*, 2004, **36**, 1018-1022.
- 63 P. A. Gerin, P. B. Dengis and P. G. Rouxhet, *Journal de chimie physique et de physico-chimie biologique*, 1995, **92**, 1043-1065.
- 64 E. Gurdak, J. Booth, C. J. Roberts, P. G. Rouxhet and C. C. Dupont-Gillain, *Journal of Colloid and Interface Science*, 2006, **302**, 475-484.
- 65 C. Liu, S. Z. Shen and Z. Han, *Journal of Bionic Engineering*, 2011, **8**, 223-233.
- 66 B. Nebe, B. Finke, F. Lüthen, C. Bergemann, K. Schröder, J. Rychly, K. Liefeth and A. Ohl, *Biomolecular Engineering*, 2007, **24**, 447-454.
- 67 G. M. Xiong, S. J. Yuan, C. K. Tan, J. K. Wang, Y. Liu, T. T. Y. Tan, N. S. Tan and C. Choong, *Journal of Materials Chemistry B*, 2014, **2**, 485-493.

Bionanocomposites of bacterial cellulose and natural hydrocolloids were developed as substrates for cell growth. There is a relation between the surface free energy of the composites and fibroblast viability. The surface properties of the bionanocomposites can be adjusted only by changing the proportions of the components.

